
Synthesis and Characterization of SnO₂/SiO₂ Nanocomposite Catalytic Material

Dr. Ajeet A. Yelwande*, Dr. M. K. Lande

Department of Chemistry, Indraraj Arts, Commerce & Science College, Sillod, Maharashtra, India.

*Department of Chemistry, Dr. Babasaheb Ambedkar Marathwada University, Aurangabad, India.

*Corresponding author

Abstract:

Nanocomposite SnO₂/SiO₂ catalytic materials have been synthesized by using sol-gel method. Prepared catalytic materials were well characterized by using transmission electron microscope (TEM), X-ray diffraction spectroscopy (XRD), scanning electron microscopy (SEM), Energy dispersive spectroscopy (EDS) and Fourier transform infrared spectroscopy (FT-IR). This prepared material will be used as heterogeneous catalytic material.

Keywords: SnO₂/SiO₂, nanocomposite, sol-gel, heterogeneous catalyst.

Introduction

A catalyst is a substance that increases the rate of a chemical reaction without itself being changed in the process. Catalysts may be in gaseous, liquid, or solid state. In homogeneous catalysis, the catalyst is molecularly dispersed in the same phase (usually gaseous or liquid) as the reactants. In heterogeneous catalysis the reactants and the catalyst are in different phases, separated by a phase boundary. Most commonly used heterogeneous catalysts are solids and the reactants are gases or liquids. On the other hand, most of the processes using homogeneous catalysts occur in a liquid phase whereas for the heterogeneous catalysts, the catalyst is usually in solid form, and the reaction occurs either in the liquid or gaseous phase. The fact that the catalyst is in a distinct phase with respect to the reaction medium, accounts for the major advantage of the heterogeneous catalysts over the homogeneous as it makes the separation techniques of heterogeneous catalysts are simple and cheap compared to the homogeneous catalysts [1].

Solid acids have been used for various chemical processes and catalytic systems because catalysis has played a major role in preventing pollution in our environment. Recently, a wide range of solid acids and their supported forms have been reported and extensively reviewed for various chemical processes [2, 3]. Owing to their possible utilizations as alternatives to liquid inorganic acids in industry, solid acid catalysts have received much consideration [4]. They have the advantages of easy separation of the catalyst from liquid reaction media, applicable recyclability, low corrosion, green chemical procedures and improved product selectivity [5]. Nanoparticles have received increasing consideration as alternative supports for catalysis. As the diameter of the particle decreases to the nanometre scale, abundant extrinsic surface becomes available for surface modifications. Furthermore, these particles can be dispersed into solvents, creating stable dispersions.

Silicates containing tin (SnO₂/SiO₂) have attracted much attention due to their surface acidity and catalytic activity in a variety of reactions such as aminolysis of styrene oxide with aniline and for the Meerwein–Ponndorf–Verley reduction of 4-tert-butylcyclohexanone [6], hydroxylation of phenols [7] Baeyer–Villiger oxidations [8] Meerwein–Ponndorf–Verley reductions [9] sugar isomerization [10] epimerization [11] oxidative dehydrogenation of cyclohexane [12] and Cannizzaro-type reactions [13].

The non-aqueous synthesis of SnO₂-SiO₂ materials is not well developed and only few reports were published on this topic. The first describes a procedure based on the reaction of TEOS with Tin(IV) acetate in anhydrous acetic acid [14]. Another report introduces the twin polymerization method for the production of SnO₂-SiO₂ materials [15]. Nanosized SnO₂ particles have been prepared by using different chemical methods such as precipitation and sol-gel [16, 17]. Tin oxide and Tin oxide supported metal oxide have been extensively used as solid acid or redox catalyst for the oxidative dehydrogenation of propane, CO oxidation, esterification reaction, reduction of NO/NO₂ to N₂ and hydrogenation reaction of nitrate [18-20]. Tin oxide has been more commonly used as a catalyst for the oxidation of organic compounds [21]. Here we wish to report, synthesis and characterization of series of SnO₂/SiO₂ as heterogeneous catalytic material.

2. Experimental section

All Chemicals were purchased either from Merck or Fluka and used without further purification. All products are known compounds and were characterized by comparing ¹H nuclear magnetic resonance (NMR) spectroscopic data and melting points with literature values. Uncorrected melting points of all compounds were measured in an open capillary in a paraffin bath. ¹H NMR spectra were recorded using a Bruker instrument (¹H at 400 MHz) in dimethyl sulfoxide (DMSO)-d₆ solvent with tetramethylsilane (TMS) as internal standard. Thin-layer chromatography (TLC) was performed with silica gel 60 F254 plates with ultraviolet (UV) light for visualization. The morphology of sample was characterized with CM-200 PHILIPS transmission electron microscopy (TEM) operated at 200 kV, resolution at 0.23 nm. FT-IR spectra were recorded on JASCO-FT-IR/4100, Japan, in KBr disc. The X-ray diffraction (XRD) patterns were recorded on Bruker 8D advance X-ray diffractometer using monochromator Cu-K radiation (40 Kv and 30 mv) of wavelength=1.5405 Å. Conventional scanning electron microscopy (SEM) images and energy dispersive spectroscopy (EDS) were obtained on JEOL; JSM-6330 LA operated at 20.0 kV and 1.0000 nA. Temperature-programmed desorption (NH₃-TPD) measurements were carried out on a Micrometrics Instrument corporation Chemisoft TPx V1.02 unit 1 (2750). The surface area of samples was characterized by the BET method performing adsorption of nitrogen at 77 K with Micrometrics ASAP 2010.

2.1 Preparation of pure silica

Silica samples were synthesized by using sol-gel process. A quantity of 2.408 gm tetraethyl orthosilicate (TEOS) was taken in autoclave bottle to which 1% Cetyl trimethyl ammonium bromide (CTAB) in 20 mL ethanol was added drop wise with constant stirring. The pH ~10 of the reaction mixture was maintained using aqueous ammonia. This mixture was then hydrothermally treated at 60°C for 12 h in an autoclavable bottle. After drying at 110°C for 7 h in an oven, the obtained powder was pulverized using mortar and pestle and finally calcined at 400°C for 2 h.

2.2 Preparation of SnO₂/SiO₂ catalyst

Series of SnO₂/SiO₂ nanocomposite catalytic materials were synthesized by using sol-gel method. Generally, 15 wt % SnO₂/SiO₂ catalysts was synthesized by using 0.846 gm of Tin(IV) chloride dissolved in 20 mL double distilled water and tetraethyl orthosilicate (TEOS) solution (2.408 gm) was added drop wise in an autoclave bottle. The resulting mixture was stirred and 1% solution of cetyltrimethylammonium bromide (CTAB) in 20 mL ethanol was added drop wise with constant stirring. The pH ~10 of the reaction mixture was maintained using aqueous ammonia. This mixture was then hydrothermally treated at 60°C for 12 h in an autoclavable bottle. After drying at 110°C for 7 h in an oven, the obtained powder was pulverized using mortar and pestle and finally calcined at 400°C for 2 h. Similarly, 10 and 20 wt % SnO₂/SiO₂ catalysts were prepared in the same manner.

3. Catalyst Characterizations

3.1 XRD Analysis

Figure 1(a-e) shows that the XRD patterns of synthesized materials. Figure 1(a) shows the broad peak at 22.27° corresponding to the amorphous nature of silica. Figure 1(b) for SnO_2 nanoparticles represent the XRD patterns for SnO_2 which shows presence of highly crystalline and sharp intense peaks, which are in good agreement with that obtained by JCPDS card no. 41-1445 [47] with lattice parameter $a = 4.743\text{\AA}$ and $c = 3.1859\text{\AA}$. The crystal planes (110), (101), (211), (002), (310), (301) were prominently seen in XRD indicating the polycrystalline nature of powder, suggesting the tetragonal lattice symmetry of this SnO_2 nano particles. There was no impurity phase was observed in all synthesized material.

Same diffraction pattern was observed for all series of $\text{SnO}_2/\text{SiO}_2$ material shown in Fig. 1(c-e). It was found that, as increasing in loading of Sn in samples, gradual increase in peaks intensity (at $2\theta = 26.60^\circ$) for the plane (110) corresponding to presence of SnO_2 . Similarly, it was found that broad peaks at 22.71° in $\text{SnO}_2/\text{SiO}_2$ corresponding to the presence of amorphous silica. From this it is clearly seen that SnO_2 crystalline nanoparticles after depositing SiO_2 on its surface enhances porosity.

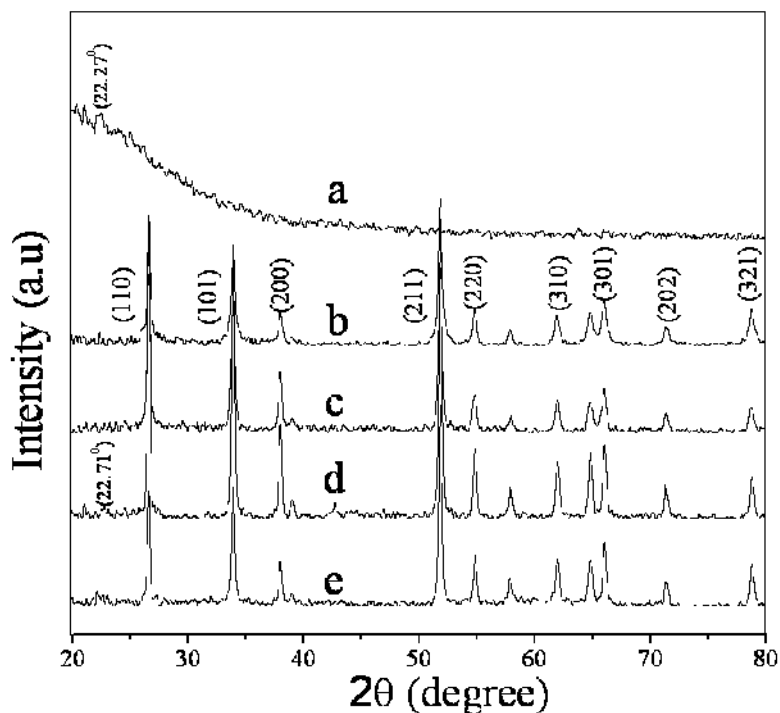


Figure 1 (a-c) XRD patterns of (a) SiO_2 (b) SnO_2 and (c) 10 wt % $\text{SnO}_2/\text{SiO}_2$ (d) 15 wt % $\text{SnO}_2/\text{SiO}_2$ (e) 20 wt % $\text{SnO}_2/\text{SiO}_2$

The average crystallite size (D) as determined from the XRD spectra using Scherrer's formula. The Scherrer equation [22] can be written as:

$$D = K \lambda / (\cos \theta)$$

Where D is the mean size of the ordered (crystalline) domains, which may be smaller or equal to the grain size; K is a dimensionless **shape factor**, with a value close to unity. The shape factor has a typical value of about 0.9; λ is the X-ray wavelength; $\Delta 2\theta$ is the line broadening at half the maximum intensity (FWHM); θ is the Bragg angle (in degrees). Average crystallite sizes of SnO_2 material was determined from 110 plane at $2\theta = 26.6^\circ$ by using Scherrer equation was shown in Table 5. It was seen that, pure sample of SnO_2 showed

crystallite sizes 12.40 nm. As loading of Sn increase, gradual decrease in crystallite sizes from 31.60 nm to 25.05 nm was observed for 10 and 15 % respectively. After that for 20% sample, small increase in crystallite size 28.35 nm was observed.

Table 1: Average crystallite sizes of SnO₂ material was determined from 110 plane by using Scherrer equation

Sr. No.	Sample	Average crystallite sizes
1	SiO ₂	-
2	SnO ₂	12.40
3	10% SnO ₂ / SiO ₂	31.60
4	15% SnO ₂ / SiO ₂	25.05
5	20% SnO ₂ / SiO ₂	28.35

3.2 TEM image

Figure 2(a-c) shows the TEM images of synthesized materials. Figure 2(a) shows the presence of varying spherical which is a characteristic property of mesoporous silica having particle size in between 288-320 nm. Figure 2(b) shows the presence of flake like SnO₂ nanoparticles with an average particle size about 7-9 nm [23]. Figure 2(c) shows that the SnO₂ nanoparticles clearly deposited on spherical shaped SiO₂ composite and therefore their particle size has ultimately reduced. This may due to the reaction between Sn(OH)₄ nanoparticle with Si(OH)₄ during the polymerization process, which results into the particle size about 25-30 nm. It is already discussed and proved in XRD. The selected area electron diraction (SAED) is a crystallographic experimental technique that can be performed inside a transmission electron microscope (TEM). The typical SAED pattern for SnO₂ nanoparticle is depicted in Figure 2(d) which indicates the presence of (110), (200), (211) and (310) planes respectively and predict the tetragonal lattice symmetry of SnO₂ nanoparticles as evidenced from XRD analysis.

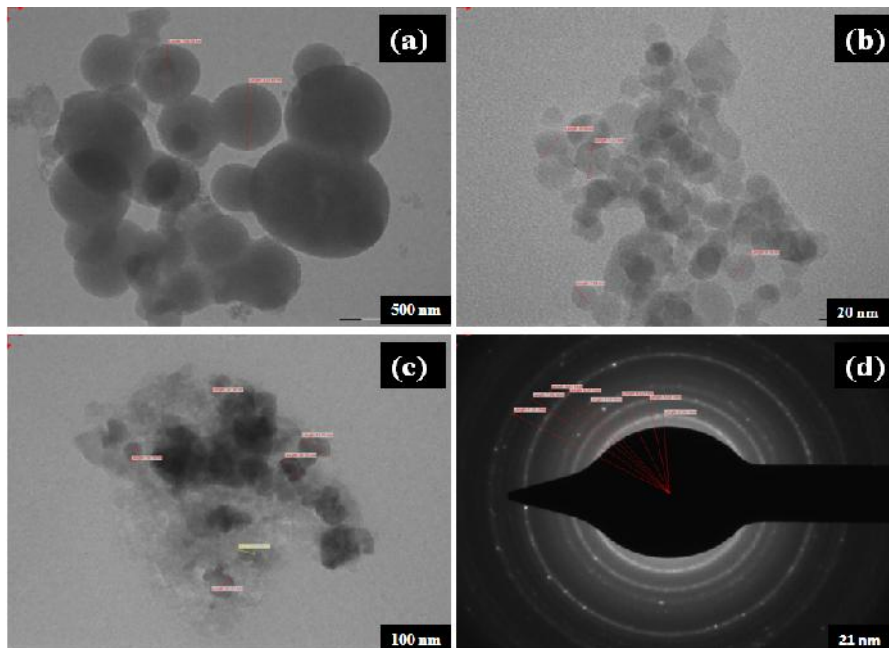


Figure 2 (a-d) TEM image of (a) SiO₂ (b) SnO₂ (c) 15 wt % SnO₂/SiO₂ (d) diffraction patterns of SnO₂

3.3 SEM-EDS analysis

Figure 3(a-c) shows the surface morphology of synthesized materials. Figure 3(a) shows good agglomeration of particles of mesoporous silica with spherical in shape, whereas a compact arrangement is due to uniform sized SnO₂ nanoparticles which are responsible for importing irregular shapes, Figure 3(b). [24] Figure 3(c-d) shows the presence of some porosity which may be due to the insertion of 15 wt % SnO₂ nanoparticles on the surface of SiO₂. This has helped in enhancing the catalytic activity of the material. Energy dispersive X-ray spectroscopy (EDS) is an analytical technique used for the elemental analysis or chemical characterization of a sample. An (EDS) spectrum of the sample with composition of 15 wt % SnO₂/SiO₂ catalysts gives the elemental distribution of the constituent elements and is represented in Figure 4. The presence of constituent elements Sn, O, and Si is confirmed on the basis of atom %, 3.65, 54.93, and 41.44 respectively. This indicates that required stoichiometric ratio in the catalyst is maintained.

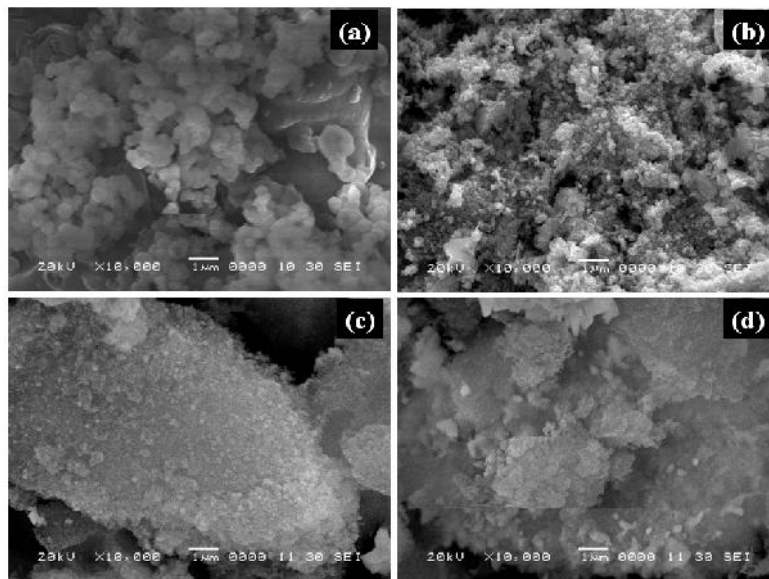


Figure 3 (a-c) SEM image of (a) SiO₂ (b) SnO₂ (c-d) 15 wt % SnO₂/SiO₂

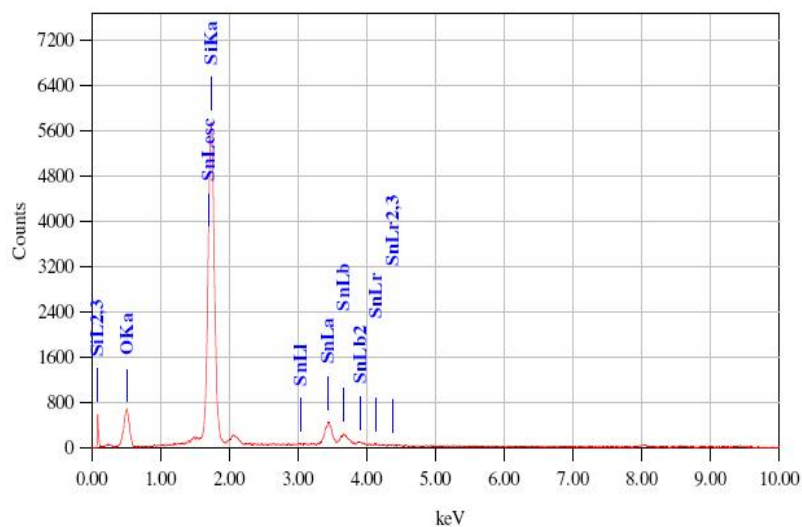


Figure 4 EDS pattern of 15 wt % SnO₂/SiO₂

3.4 FTIR Analysis

10 mg of dry sample was ground with oven dry KBr (200 mg) the resulting homogeneous mixture 100 mg was taken in sample holder. The prepared sample was put in JASCO-FT-IR/4100, spectrometer and scanned between IR ranges of 4000-400 cm^{-1} . In Figure 5(a-e) shows the FT-IR spectra of the synthesized materials. Figure 5(a) shows the FT-IR spectrum of pure SnO_2 having absorption band at 3205 cm^{-1} which is due to the Sn-OH stretching vibration, and the band at 1634 cm^{-1} is assigned for the Sn-OH bending vibration. Figure 5(b) shows the FT-IR spectrum of pure SiO_2 gives absorption band at 3410 cm^{-1} due to the Si-OH stretching vibration, 1618 cm^{-1} due to the Si-OH bending mode, 1089 cm^{-1} for Si-O stretching vibration and 806 cm^{-1} due to the Si-O-Si bending vibrational mode. The strong absorption band at 631 cm^{-1} is due to the antisymmetric Sn-O-Sn vibrational mode of SnO_2 . The similar results were reported in the literature by Deshpande et al [25]. Similarly Figure 5(c-e) shows that the absorption bands at 3408, 1620, 1093, 806 and 631 cm^{-1} are attributed to the $\text{SnO}_2/\text{SiO}_2$ framework.

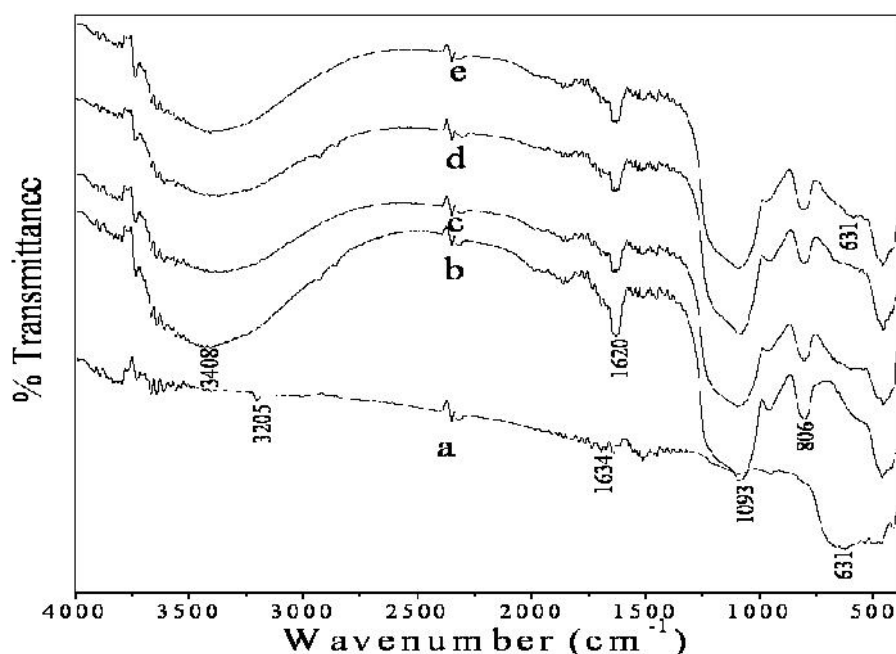


Figure 5 (a-c) FT-IR patterns of (a) SnO_2 (b) SiO_2 (c) 10 wt % $\text{SnO}_2/\text{SiO}_2$ (d) 15 wt % $\text{SnO}_2/\text{SiO}_2$ (e) 20 wt % $\text{SnO}_2/\text{SiO}_2$

3.5 TPD analysis

NH_3 -TPD measurements were carried out by (i) pre-treating of samples from room temperature to 150°C in Helium flow 25 cc/min for 1 hour; (ii) adsorption of ammonia at room temperature; (iii) Desorption of adsorbed ammonia with an heating rate 10°C min^{-1} starting from the adsorption temperature from 50 to 500°C. The NH_3 -TPD desorption provides information about the total concentration and strength of acidic sites present in materials. The total acidity of 15 wt% $\text{SnO}_2/\text{SiO}_2$ material is found 0.149 mmol/gm shown in Table 1, clearly indicate presence of Brønsted acidic sites, which help to increases catalytic activity of material.

Table 2 The acid strength and surface area

Entry	Catalyst	Total acidity (mmol/gm)	Surface area (m^2/gm)
1	15 wt % $\text{SnO}_2/\text{SiO}_2$	0.149	331.58

3.6 Brunauer-Emmett-Teller surface area (BET)

The N₂-BET surface areas of 15 wt% SnO₂/SiO₂ material were characterized and shown in Table 1. The amount of N₂ gas adsorbed-desorbed at a given pressure allows determining the surface area of material. The isotherm for prepared material indicates large volume was adsorbed on surface of material. The BET surface area observed is 331.58 m²/gm. It indicates material has large surface area and hence this material shows higher catalytic activity.

Conclusion

In summary, an efficient heterogeneous catalytic system has been developed. Nanocomposite SnO₂/SiO₂ catalytic materials have been synthesized by using sol-gel method. Prepared catalytic materials were well characterized by using transmission electron microscope (TEM), X-ray diffraction spectroscopy (XRD), scanning electron microscopy (SEM), Energy dispersive spectroscopy (EDS) and Fourier transform infrared spectroscopy (FT-IR). This prepared material will be used as heterogeneous catalytic material.

Acknowledgements

The authors are thankful to the Head, Department of Chemistry, Jijamata College of Science and Arts, Bhende bk, Ahmednagar, Maharashtra, 414605, India for providing the laboratory facility.

References

1. Encyclopedia britannica online, 2004.
2. P. Gupta, S. Paul, Catal. Today 2014, 236, 1530.
3. M. Kaur, S. Sharma, P. M. S. Bedi, Chin. J. Catal. 2015, 36, 520.
4. a) M. E. Davis, Nature 2002, 417, 813; b) A. Corma, H. Garcia, Chem. Rev. 2003, 103, 4307; c) W. P. Wong, L. Y. S. Lee, K. M. Lam, Z. Y. Zhou, T. H. Chan, K. Y. Wong, ACS Catal. 2011, 1, 116.
5. a) M. Choi, K. Na, J. Kim, Y. Sakamoto, O. Terasaki, R. Ryoo, Nature 2009, 416, 246; b) E. Nikolla, Y. Roman-Leshkov, M. Moliner, M. E. Davis, ACS Catal. 2011, 1, 408; c) P. Barbaro, F. Liguori, Chem. Rev. 2009, 109, 515.
6. David Skoda, Ales Styskalik, Zdenek Moravec, Petr Bezdicka, Jiri Bursik, P. Hubert Mutine and Jiri Pinkas, RSC Adv., 2016, 6, 68739.
7. X. Wang, H. Xu, X. Fu, P. Liu, F. Lefebvre and J.-M. Basset, J. Mol. Catal. A: Chem., 2005, 238, 185–191.
8. A. Corma, M. A. T. Navarro and M. Renz, J. Catal., 2003, 219, 242–246.
9. A. Corma, M. E. Domine and S. Valencia, J. Catal., 2003, 215, 294–304.
10. H. J. Cho, P. Dornath and W. Fan, ACS Catal., 2014, 4, 2029–2037.
11. W. R. Gunther, Y. Wang, Y. Ji, V. K. Michaelis, S. T. Hunt, R. G. Griffin and Y. Rom'an-Leshkov, Nat. Commun., 2012, 3, 1109.
12. S. Samanta, N. K. Mal, A. Manna and A. Bhaumik, Appl. Catal., A, 2004, 273, 157–161.
13. E. Taarning, S. Saravanamurugan, M. Spangenberg Holm, J. Xiong, R. M. West and C. H. Christensen, ChemSusChem, 2009, 2, 625–627.
14. P. Kirszenstejn, A. Kawałko, A. Tolińska and R. Przekop, J. Porous Mater., 2010, 18, 241–249.
15. C. Leonhardt, S. Brumm, A. Seifert, G. Cox, A. Lange, T. Ruffer, D. Schaarschmidt, H. Lang, N. Jöhrmann, M. Hietschold, F. Simon and M. Mehring, ChemPlusChem, 2013, 78, 1400–1412.
16. Antonio, J. A. T.; Baez, R. G.; Sebastian, P. J.; Vazquez, A. Thermal stability and structural deformation of rutile SnO₂ nanoparticles. *J. Solid state Chem.* 2003, 174, 241–248.
17. Zhang, J.; Gao, L. Synthesis and characterization of nanocrystalline tin oxide by sol-gel method. *J. Solid State Chem.* 2004, 177, 1425–1430.
18. Hagemeyer, A.; Hogan, Z.; Schlichter, M.; Smaka, B.; Streukens, G.; Turner, H.; Volpe, J. A.; Weinberg, H.; Yaccato, K. High surface area tin oxide. *Appl. Catal. A. Gen.* 2007, 317, 139–148.
19. Khder, A. E. R. S. Preparation, characterization and catalytic activity of tin oxide-supported 12-tungstophosphoric acid as a solid catalyst. *Appl. Catal. A. Gen.* 2008, 343, 109–116.

-
20. Li, J.; Hao, J.; Fu, L.; Liu, Z.; Cui, X. The activity and characterization of sol–gel Sn/Al₂O₃ catalyst for selective catalytic reduction of NO₂ in the presence of oxygen. *Catal. Today* 2004, *90*, 215-221.
 21. Kawabe, T.; Tabata, K.; Suzuki, E.; Ichikawa, Y.; Nagasawa, Y. Morphological effects of SnO₂ thin film on the selective oxidation of methane. *Catal. Today* 2001, *71*, 21-29.
 22. Scherrer, P. *Göttinger Nachrichten Gesell.* **1918**, *2*, 98–100.
 23. Gnanam, S.; Rajendran, V. Anionic, cationic and nonionic surfactants-assisted hydrothermal synthesis of tin oxide nanoparticles and their photoluminescence property. *Digest Journal of Nanomaterials and Biostructure s.* 2010, *5*,623-628.
 24. Wang, Yu-de.; Ma, Chun-lai.; Sun, Xiao-dan.; Li, Hang-de. Preparation and characterization of SnO₂ nanoparticles with a surfactant-mediated method. *Nanotechnology.* 2002, *5*, 565-569.
 25. Deshpande, N. G.; Gudage, Y. G.; Sharma, R.; Vyas, J. C.; Kim, J. B.; Lee, Y. P. Studies on tin oxide intercalated polyaniline nanocomposite for ammonia gas sensing applications *Sensors and Actuators B: Chemical* 2009, *138*,76–84.